Article:

Zhao, B., Dai, Q., Zhuo, L. orcid.org/0000-0002-5719-5342 et al. (3 more authors) (2021) Assessing the potential of different satellite soil moisture products in landslide hazard assessment. Remote Sensing of Environment, 264. 112583. ISSN 0034-4257

https://doi.org/10.1016/j.rse.2021.112583

Assessing the potential of different satellite soil moisture products in landslide hazard assessment

Binru Zhao[1,2], Qiang Dai[1,2,3], Lu Zhuo[4], Shaonan Zhu[5], Qi Shen[1], Dawei Han[3]

[1]Key Laboratory of VGE of Ministry of Education, Nanjing Normal University, Nanjing, China.

[2]Jiangsu Center for Collaborative Innovation in Geographical Information Resource Development and Application, Nanjing, China.

[3]Department of Civil Engineering, University of Bristol, Bristol, UK.

[4]Department of Civil and Structural Engineering, the University of Sheffield, Sheffield, UK.

[5]College of Geographical and Biological Information, Nanjing University of Posts and Telecommunications, Nanjing, China.

Corresponding author: Qiang Dai (qiangdai_nnu@163.com)

Keywords

satellite soil moisture; landslide; soil moisture variability; SMAP

Abstract

With the development of remote sensing technology, satellite-based soil moisture estimates become more and more available, and the potential of using satellite soil moisture products in landslide hazard assessment has been widely recognized. However, to our knowledge, there is a lack of studies exploring the performance difference of various satellite soil moisture products for such an application. Therefore, this study aims to compare several state-of-the-art satellite soil moisture products on their potentials in landslide applications. The selected products include the ESA CCI soil moisture dataset, the SMAP Level-3 (L3), enhanced Level-3 (L3), Level-4 (L4) surface, and Level-4 (L4) root zone soil moisture datasets. Specifically, the completeness of different datasets is calculated to assess their applicability in practical applications. To investigate the relationship between the soil moisture and the commonly used rainfall information in landslide predictions, the correlation study of the satellite soil moisture with the antecedent cumulated rainfall is also carried out. In addition, to explore whether the satellite soil moisture can provide valuable information for landslide hazard assessment, infiltration events are identified based on the time series of satellite soil moisture, and the significance of event characteristics (such as event duration, soil moisture change, etc.) in landslide occurrence is then investigated with Bayesian analysis. This study is carried out in a landslide-prone area, the Emilia-Romagna region in northern Italy. Results show that the SMAP L4 product does not have any missing values, beneficial to the continuous monitoring of landslides. As for the correlation relationship between soil moisture and antecedent cumulated rainfall, the SMAP L4 product also has more rational spatial distribution of the Pearson correlation coefficients compared with other datasets, which can be better explained by the distribution of slope and TWI (topographic wetness index). Bayesian analysis on the infiltration events shows that our prior knowledge of the probability of landslide occurrence is better improved by using the 'SMAP L4 root zone soil moisture'-derived infiltration events, indicating its greater potential to be used for landslide hazard assessment in the study region.

1. Introduction

As one of the most common and frequent natural hazards, landslides pose great threats to human lives and infrastructures. With the increasing development of mountainous areas, people and infrastructures are becoming more exposed to landslides. The increase of extreme rainfall events caused by climate change also increases the frequency of rainfall-triggered landslides. These make the threats from landslides more serious.

To mitigate the impact of landslides, a landslide early warning system (LEWS) is essential to notify the public of upcoming landslides in the hazard regions all over the world (Lagomarsino et al. 2012; Naidu et al. 2018;

Piciullo et al. 2018; Segoni et al. 2018). From the published literature, LEWS is mainly based on traditional statistical approaches, like the commonly used rainfall thresholds. Although LEWS performs well in terms of high hit rate, it is usually achieved at the cost of high false alarm rates (Gariano et al. 2019; Rosi et al. 2016). Based on the rationale that landslides are initiated by the increase in pore water pressures, which is more related to soil moisture, some scholars attempted to improve the credibility of LEWS by making use of the soil moisture information (Glade et al. 2000; Godt et al. 2006; Thomas et al. 2019; Zhao et al. 2019; 2020). For instance, Marino et al. (2020) defined hydro-meteorological thresholds with the soil moisture and rainfall information, and the false alarm rate of LEWS was significantly reduced. Besides combining with rainfall information, soil moisture is also directly used to provide valuable information for landslide early warnings. For example, Zhuo et al. (2019b) developed soil moisture thresholds for landslides monitoring under varied environmental conditions including land cover, soil type and slope. Wicki et al. (2020) used soil moisture as a proxy for landslide occurrences, and demonstrated the potential of soil moisture measurements for regional landslide early warning.

In-situ measurements could provide accurate soil moisture information; however, due to the high cost of instruments and maintenance, it is difficult to have dense measurement networks over large areas. There are only a few studies that have explored the potential of using in-situ soil moisture measurements for landslide early warnings (Mirus et al. 2018a; 2018b; Thomas et al. 2020). Land surface modelling or hydrological modelling is another way to estimate soil moisture. Zhuo et al. (2019a) integrated three advanced Land Surface Model schemes with the Weather Research and Forecasting (WRF) model to estimate soil moisture for landslide hazard assessment. Zhao et al. (2020) used a distributed hydrological model SHETRAN to simulate soil moisture, and applied it to define thresholds for landslide predictions. However, limitations persist for these modelling approaches due to the high demand for accurate data inputs. Soil moisture information could also be retrieved using remote sensing technology, which is a major source of large-scale dataset that is available globally. There are many satellites in orbit providing soil moisture estimates. Some are specifically dedicated to the measurement of soil moisture from space, like the Soil Moisture Ocean Salinity (SMOS) mission by the European Space Agency (ESA), and the Soil Moisture Active Passive (SMAP) mission by the National Aeronautics and Space Administration (NASA); Others provide soil moisture estimates by carrying onboard sensors, like the Advanced Scatterometer (ASCAT) on the ESA's MetOp-A and MetOp-B satellites, and the Advanced Microwave Scanning Radiometer 2 (AMSR2) on the Japan Aerospace Exploration Agency (JAXA)'s GCOM-W1 satellite. Extended from these measurements, there are various satellite-based soil moisture products available for research and operational purposes, such as the ESA Climate Change Initiative (CCI) soil moisture product derived by merging multiple active and passive sensors (https://www.esa-soilmoisture-cci.org/), and the SMAP Level-3 (L3), enhanced Level-3 (L3), Level-4 (L4) surface and root zone soil moisture products derived from the estimates of the SMAP passive microwave radiometer (https://smap.jpl.nasa.gov/data/). With the availability of satellite-based soil moisture estimates, there is an increasing interest in the possibility of using such datasets for landslide hazard assessment. For instance, Brocca et al. (2016) used satellite soil moisture product ASCAT to improve the prediction of landslide hazard for an operational early warning system in Umbria Region (central Italy). Thomas et al. (2019) assessed the feasibility of satellite-based information in the definition of thresholds for landslides, and demonstrated the utility of the SMAP L4 root zone product for LEWS. Felsberg et al. (2021) carried out a global feasibility study to explore the effectiveness of SMOS, SMAP, and GRACE observations, land surface simulations, and data assimilation for the probabilistic modeling of hydrologically triggered landslides. The authors pointed out that the SMAP L4 product was generally more beneficial than the others for the landslide applications.

Despite a number of studies that have demonstrated the potential of using satellite soil moisture in landslide hazard assessment, few have evaluated and compared the difference in this potential for various satellite soil moisture products. Due to differences in satellite sensors, scan pattern, revisit period and processing algorithms, satellite-based soil moisture products vary greatly in accuracy and resolutions, which has been widely explored in studies of comparing different satellite soil moisture products (Al-Yaari et al. 2019; Cui et al. 2017; Ma et al. 2019). It could be inferred that these different characteristics will lead to different potentials for landslide applications. Therefore, we aim to assess the potential of several state-of-the-art satellite soil moisture products for landslide hazard assessment, which can provide a relevant and timely contribution filling in a critical knowledge gap in the field and further prompt the use of satellite soil moisture in landslide researches. In this study, five satellite soil moisture datasets are selected, including the ESA CCI soil moisture dataset, the SMAP Level-3 (L3), enhanced Level-3 (L3), Level-4 (L4) surface, and Level-4 (L4) root zone soil moisture datasets. The reason for considering the ESA CCI soil moisture dataset is that it is created by merging information from multiple active and passive sensors. SMAP soil moisture datasets are selected because SMAP operates at L-band whereas AMSR-E and ASCAT retrievals are based on X-band (10.7 GHz) and C-band (5.3 GHz), respectively, and microwave radiometry at L-band (1.4-1.427 GHz) is recognized as a better solution for soil moisture estimation (Monerris et al. 2009). Besides, compared with SMOS that also uses L-band, SMAP could offer observations at a higher spatial resolution that are less affected by radiofrequency interference than those from SMOS. We assess these satellite soil moisture products from the perspective of their application in landslide hazard assessment, specifically focusing on three aspects: (1) the completeness of the datasets is calculated to assess their applicability in practical applications; (2) to investigate the relationship between the soil moisture and the commonly used rainfall information in landslide predictions, the correlation study of satellite soil moisture with antecedent cumulated rainfall is carried out; (3) to explore the potential of satellite soil moisture in providing valuable information for landslide hazard assessment, infiltration events are identified based on the time series of satellite soil moisture data, and the significance of event characteristics in landslide occurrence is investigated with Bayesian analysis. The study area is the Emilia-Romagna region (northern Italy), which is an extensively studied landslide-prone region due to its abundant landslide records, and rich measurements of the hydrological and meteorological information.

2. Study area and data sources

2.1 Study area

The study area is the Emilia-Romagna region in the north of Italy, covering an area of approximately 22446 square kilometers (Figure 1). The north and east of this region are flat, formed by alluvial deposits of the Po River. The southern and western parts are occupied by hills and mountains of Apennines, with the maximum altitude reaching 2165m. The mountainous area is highly subject to landslide hazards of different types, such as rational-translational slides, slow earth flows and complex movements. Landslides are mainly induced by rainfall in this region. Corresponding to the characteristics of the Mediterranean climate (warm and dry summer, and mild/cold and wet winter), rainfall-triggered landslides occur frequently in autumns and winters.

2.2 Landslide data

Landslide data used in this study are provided by the Emilia-Romagna Geological Survey, which collects landslide information from various sources, such as researches, reports, national and local press, technical documents, etc. The recorded landslide information should include the occurrence location, location accuracy, occurrence date, date accuracy, landslide characteristics (length, width, type and material), triggering factors, damage and references. Since landslides mainly occur in mountainous areas, it is difficult to collect all the information. As a result, in most cases, only the occurrence location, location accuracy, date and date accuracy were recorded. Despite these issues, this landslide catalogue is relatively complete compared with other regions. We only select landslides that have good confidence in occurred location and date for analysis. There are 292 qualified landslides for the study period from April 2015 to December 2019, marked with pushpins in Figure 1.

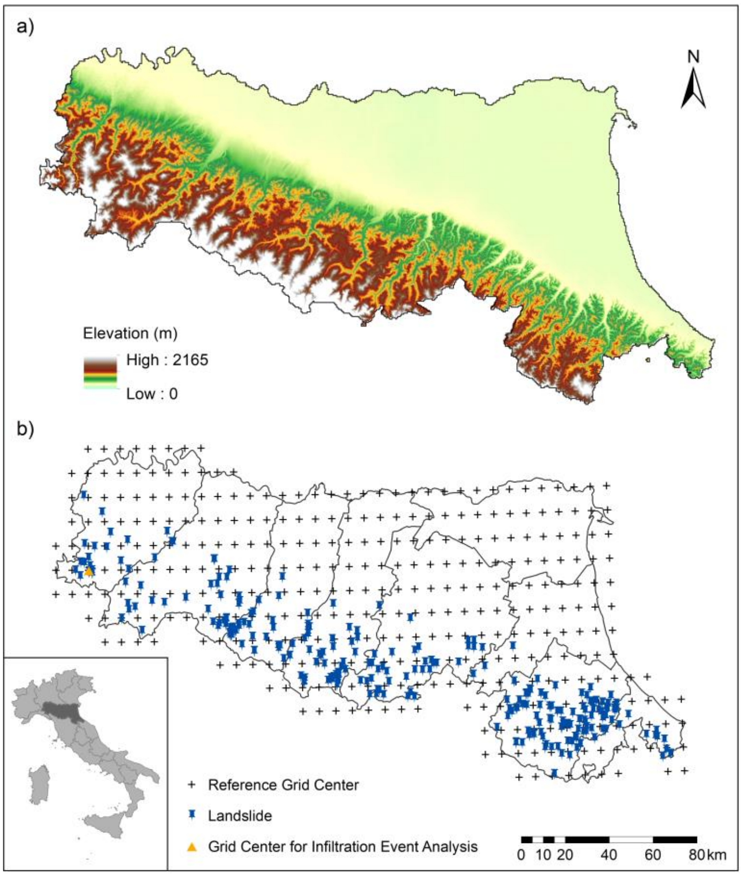

Figure 1. Map of the Emilia-Romagna region and the location of reference grid centers, landslides, and the grid center for infiltration event analysis.

2.3 Rainfall data

The rainfall data used in this study are from the ERG5 dataset provided by the Regional Agency for Prevention, Environment and Energy of Emilia-Romagna (Arpae) (https://dati.arpae.it/dataset/erg5-interpolazione-su-griglia-di-dati-meteo). The ERG5 dataset includes hourly and daily data for the main meteorological and agro-meteorological variables, such as air temperature, precipitation, relative air humidity, solar irradiance and wind. This dataset is obtained by spatial interpolation on a regular grid starting from the values detected by the network of historical meteorological stations, covering the whole territory of the Emilia-Romagna region from 2001 to today.

2.4 Satellite soil moisture products

Five latest satellite soil moisture datasets are selected for analysis in this study, which are from for the ESA CCI soil moisture product and the SMAP soil moisture product.

The ESA CCI soil moisture product is from the ESA Program on Global Monitoring of Essential Climate Variables (ECV), which is initiated in 2010 and produces an updated soil moisture product every year (Dorigo et al. 2017). There are three separate soil moisture products derived from active, passive and combined (active + passive) sensors. The ACTIVE product and the PASSIVE product were created by fusing scatterometer and radiometer soil moisture products, respectively; and the COMBINED product was created by blending the former two datasets. In this study, we use the COMBINED product of the latest version (v05.2). Compared with the previous versions, this version firstly includes SMAP radiometer data. Other improvements include improved intercalibration of AMSR-2 in the PASSIVE product and improved retrieval algorithm for all PASSIVE sensor data. The format of the ESA CCI soil moisture is in the volumetric water content (m^3/m^3), with a spatial resolution of 0.25 degree and a daily temporal resolution.

SMAP is a NASA environmental monitoring satellite launched on 31 January 2015, which is the latest on-orbit satellite specifically dedicated to the measurement of soil moisture (Piepmeier et al. 2017). SMAP carries two instruments, a radiometer (passive) and a synthetic-aperture radar (active). The approach of combing active and passive measurement takes advantage of the spatial resolution of the radar and the sensing accuracy of the radiometer. There are four levels of data processing: Level 1 products contain instrument-related data; Level 2 products result from geophysical retrievals that are based on instrument data; Level 3 products are daily global composites of the Level 2 geophysical retrievals for an entire UTC day, which are derived by re-sampling the Level 2 product to a global grid; Level 4 products contain estimates of root zone soil moisture, which are obtained by assimilating SMAP observations into a land surface model. In this study, three SMAP products are adopted for analysis: (1) SMAP L3 Radiometer Global Daily 36 km EASE-Grid Soil Moisture, Version 7 (hereinafter referred to as 'SMAP-P'); (2) SMAP Enhanced L3 Radiometer Global Daily 9 km EASE-Grid Soil Moisture, Version 4 (hereinafter referred to as 'SMAP-PE'); (3) SMAP L4 Global 3-hourly 9 km EASE-Grid Surface and Root Zone Soil Moisture Geophysical Data, Version 5, including surface soil moisture and root zone soil moisture (hereinafter referred to as 'SMAP-Sur' and 'SMAP-RZ', respectively). The format of these four datasets is also in the volumetric water content (m^3/m^3).

Table 1 shows the detailed information of these satellite soil moisture products. For a fair comparison, we make the spatial and temporal resolution of these products consistent. The 9 km grid of the SMAP-PE dataset is used as the reference grid to which all satellite products are interpolated through the nearest neighboring method (reference grid centers are shown in Figure 1). The adopted temporal resolution is one day, at which the 3-hourly SMAP-Sur and SMAP-RZ datasets are aggregated. Considering the common temporal coverage of the selected datasets, the study period is from April 2015 to December 2019.

Table 1. Detailed information of satellite soil moisture datasets.

Product	Abbreviation	Temporal coverage	Temporal resolution	Spatial resolution	Soil depth
ESA CCI COMBINED soil moisture product (v05.2)	ESA CCI	11. 1978 to 12. 2019	daily	0.25° x 0.25°	0-5cm
SMAP L3 Radiometer Global Daily 36 km EASE-Grid Soil Moisture (v7)	SMAP-P	4.2015 to present	daily	36 km x 36km	0-5cm

SMAP Enhanced L3 Radiometer Global Daily 9 km EASE-Grid Soil Moisture (v4)	SMAP-PE			9 km x 9 km	0-5cm
SMAP L4 Global 3-hourly 9 km EASE-Grid Surface and Root Zone Soil Moisture Geophysical Data (v5)	SMAP-Sur		3-hourly	9 km x 9 km	0-5cm
	SMAP-RZ				0-100cm

3. Methods

3.1 Data pre-processing

As the satellite soil moisture estimates in terms of volumetric water content range from 0 to 1 m^3/m^3, values outside this range are firstly marked as outliers. Although in most cases missing values are tagged, there are datasets with untagged missing values. Therefore, we first search the untagged missing values, and then replace all the missing values and outliers with a ‘na’ tag.

After the quality control, the time series of soil moisture in terms of the volumetric water content is normalized with the minimum and maximum value for three reasons. First, owing to the limited knowledge of the local soil conditions, there are uncertainties related to the sensor calibration, which would lead to uncertainties associated with the absolute value of the volumetric water content. Second, the difference in the variation range due to the spatial heterogeneity makes it difficult to carry out analyses. Third, in landslide research, soil saturation has been used as an indicator of predicting landslide occurrence (Mirus et al. 2018b), and soil saturation is more related to the relative soil moisture than the absolute value of volumetric water content. The min-max normalization uses the following equation:

$$\theta_{norm} = \frac{\theta - \theta_{min}}{\theta_{max} - \theta_{min}} \quad (1)$$

where θ, θ_{max} and θ_{min} are the measured, maximum and minimum value of the volumetric water content of the individual time series, respectively. The soil moisture mentioned in the analysis of the infiltration events refers to the normalized soil moisture.

3.2 Infiltration events

To evaluate the performance of satellite soil moisture product in providing valuable information for landslide assessment, infiltration events are identified and characterized. The continuous increase of soil moisture caused by the infiltration process is regarded as the infiltration event.

An automatic algorithm is designed to identify infiltration events based on satellite soil moisture estimates and quantify the conditions that characterize an infiltration event.

Step 1: Identification of infiltration events

With the pre-processed data, the soil moisture variation rate per day is calculated. The algorithm starts by searching for the variation rate smaller than the threshold T_1, referred to as the minor fluctuation. If the direction of the minor fluctuation is opposite to its neighbors before and after, the minor fluctuation is marked as the inverse minor fluctuation. The inverse minor fluctuations are considered as noise, and the algorithm multiplies these variations rates by -1. The algorithm then searches for the period of continuous increase of the soil moisture variation rate, and the detected periods are infiltration events. To avoid the effect of other factors like the measurement noise and temperature effects, infiltration events that have a total increase rate smaller than the threshold T_2 are removed.

T_1 and T_2 are determined automatically for each time series of the soil moisture. In this study, values less than the 10th percentile are regarded as noise. Therefore, T_1 is determined as the 10th percentile of the soil moisture variation rate per day, and T_2 is determined as 10th percentile of the increase rate of the infiltration event.

Step 2: Quantification of infiltration event characteristics

Six indicators are calculated to characterize the infiltration event, including infiltration duration, start soil moisture, maximum soil moisture, mean soil moisture, soil moisture change from the start to the end and rate of soil moisture change (soil moisture change divided by the event duration).

As the spatial resolution of the interpolated satellite soil moisture is 9 km, landslides within a 5 km radius are searched for each infiltration event. Thus, infiltration events are classified into two categories: infiltration events with landslides and infiltration events without a landslide. For infiltration events with landslides, the characteristics are re-calculated by truncating the event on the day the landslide occurs.

3.3 Bayesian analysis

Univariate Bayesian analysis is applied to assess the significance of infiltration event characteristics in landslide occurrence and the corresponding differences between different satellite soil moisture products. Univariate Bayesian analysis is based on the definition of the conditional probability $P(L|I_c)$, which is the probability of landslide occurrence given a certain characteristic I_c of the infiltration event:

$$P(L|I_c) = \frac{P(I_c|L) \cdot P(L)}{P(I_c)} \quad (2)$$

where $P(L)$ is the prior probability of landslides, defined as the number of landslide-related infiltration events divided by the total number of infiltration events; $P(I_c)$ is the probability that a certain characteristic I_c falls within a given interval, defined as the number of infiltration events that a certain characteristic I_c falling within a chosen interval, divided by the total number of infiltration events; $P(I_c|L)$ is the conditional probability of a certain characteristic I_c given landslide occurrence, calculated in the same way as $P(I_c)$, but only considering infiltration events with landslides.

In Bayesian terms, the comparison between $P(L|I_c)$ and $P(L)$ indicates how our prior knowledge of the probability of landslide occurrence is improved by the additional information provided by a certain characteristic of infiltration events.

4. Results

4.1 Completeness evaluation

In landslide research, the analysis based on soil moisture information highly relies on the continuity of data. However, due to the technical and operational problems, there are typically missing values in the dataset. Although individual missing values have little effect on the effectiveness of information, multiple and intermittent missing values could result in loss of information and affect the applicability of data. Therefore, the completeness of different satellite soil moisture datasets is first evaluated by analyzing the missing values. Figure 2 shows the boxplot of missing values for different satellite soil moisture datasets at all the reference grid cells for the period from 1 April 2015 to 31 December 2019. As SMAP L4 is a modeled product, it is not surprising that SMAP-Sur and SMAP-RZ have the continuous data, without any missing value. The proportion of missing values for ESA CCI varies greatly for different locations, with a median of 9%. The variation of missing values for SMAP-P and SMAP-PE is small, where the proportion of missing values fluctuates around 50%. Besides, through inspecting the distribution of missing values in the dataset, it is found that the missing values in the ESA CCI dataset are individual and occasional, while the missing values are interspersed in the SMAP-P and SMAP-PE datasets, with one missing value for every one or two records.

Although the proportion and distribution of missing values of ESA CCI have a minor impact on the analysis of time series, it is within an acceptable range. However, for SMAP-P and SMAP-PE, the large missing values interspersed between records make it difficult to analyze the temporal variation of soil moisture and provide valuable information for landslide occurrence. In this study, the missing values of SMAP-P and SMAP-PE product hinder the identification of infiltration events. Therefore, in the following analysis on the infiltration events, the SMAP-P and SMAP-PE products are omitted.

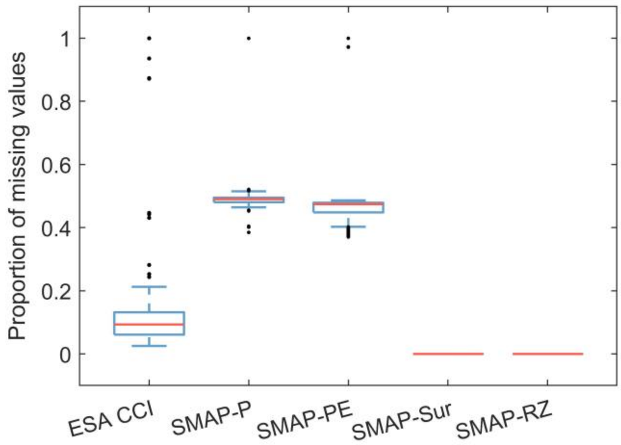

Figure 2. Boxplot representations of the median (red line), upper and lower quartiles (box), 1.5Â interquartile range (whiskers) and outliers (black dots) for missing values at all the reference grid cells for the period from 1 April 2015 to 31 December 2019.

4.2 The correlation with antecedent cumulated rainfall

The temporal variation of soil moisture relies on the change of meteorological conditions, especially rainfall conditions. And also because of the easier availability of rainfall information, the antecedent cumulated rainfall is usually used as an indirect proxy of soil moisture in the prediction of landslide occurrences. As soil moisture information becomes more and more accessible, it is suggested to directly use soil moisture information in landslide predictions. To investigate the relationship between the soil moisture and the commonly used rainfall information, we calculated the Pearson correlation coefficient (r) between the soil moisture and the antecedent cumulated rainfall, which is shown with boxplots in Figure 3, with the consideration of different durations of the antecedent period. For ESA CCI, SMAP-P, SMAP-PE and SMAP-Sur, the value of r grows with the increase of the antecedent days, and reaches the best performance when the duration of the antecedent period is 30 days, after which the value of r becomes smaller again. For SMAP-

RZ, soil moisture has the best correlation relationship with the antecedent 60-day cumulated rainfall. It is obvious that the soil moisture is correlated with the antecedent cumulated rainfall, which explains why antecedent cumulated rainfall has been used with some successes for landslide predictions in previous studies. However, it should be noted that even for the best performance at the antecedent 30-day (or 60-day) cumulated rainfall, the value of r is not high, with a median less than 0.6. This is expected, because in addition to rainfall, there are other factors controlling the variation of soil moisture, such as evapotranspiration and lateral flow.

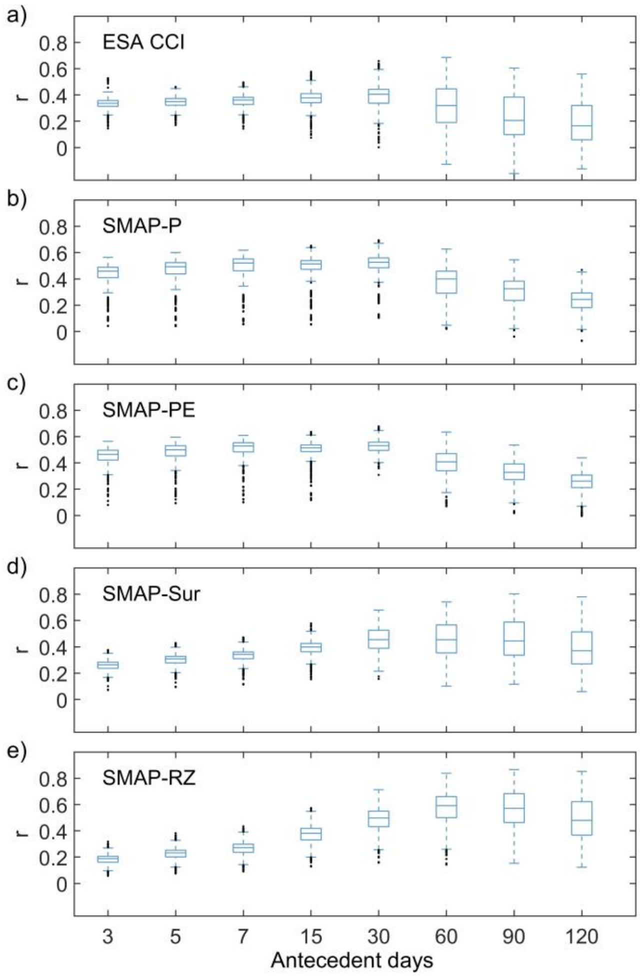

Figure 3. Boxplot representations of the median (red line), upper and lower quartiles (box), 1.5Â interquartile range (whiskers) and outliers (black dots) for the Pearson correlation coefficient (r) between soil moisture and antecedent cumulated rainfall at all the reference grid cells.

The spatial distribution of the Pearson correlation coefficient (r) between the soil moisture and the antecedent cumulated rainfall is further explored, as shown in Figure 4, where the antecedent period is 30 days for ESA CCI, SMAP-P, SMAP-PE and SMAP-Sur, and 60 days for SMAP-RZ. From Figure 4, for most grid cells, the value of r varies largely for different soil moisture datasets. For example, for grid cells at the southwest of the Emilia-Romagna region, the value of r ranges from 0.4 to 0.5 for ESA CCI, and from 0.5 to 0.6 for SMAP-P, SMAP-PE and SMAP-Sur, while the value of r is greater than 0.6 for SMAP-RZ. Although the five satellite soil moisture datasets have differences in the value of r for the same grid cell, their spatial distribution of r exhibits a similar pattern. The value of r generally increases from the northeast to the southwest.

To explain this pattern, we investigate the topographic control on the spatial distribution of the correlation coefficients by considering the elevation, slope and topographic wetness index (TWI). TWI is defined as $\ln(\alpha/\tan\beta)$, where α is the local upslope area draining through a certain point and $\tan\beta$ is the local slope (Beven and Kirkby 1979). Given the correlation coefficient is based on the grid cell, the average value of the topographic indicators (elevation, slope and TWI) is also calculated for each grid cell. Figure 5 shows the scatter plots of the Pearson correlation coefficient (r) against topographic indicators for the five satellite soil moisture datasets. For ESA CCI, SMAP-P and SMAP-PE, there is no obvious relationship between Pearson's r and the topographic indicators in terms of elevation, slope and TWI. For SMAP-Sur and SMAP-RZ, the slope correlate positively with Pearson's r, while TWI correlates negatively with r. The opposite relationship for slope and TWI is reasonable, because TWI has a negative relationship with slope. When TWI is larger, the lateral flow has an important role in the variation of soil moisture in addition to the antecedent rainfall, which could lead to a smaller r between the soil moisture and the antecedent cumulated rainfall. Therefore, TWI is expected to have a negative correlation with r. Moreover, given the negative relationship between TWI and slope, the slope is expected to have a positive correlation with r. From this point, SMAP-Sur and SMAP-RZ perform better than other datasets.

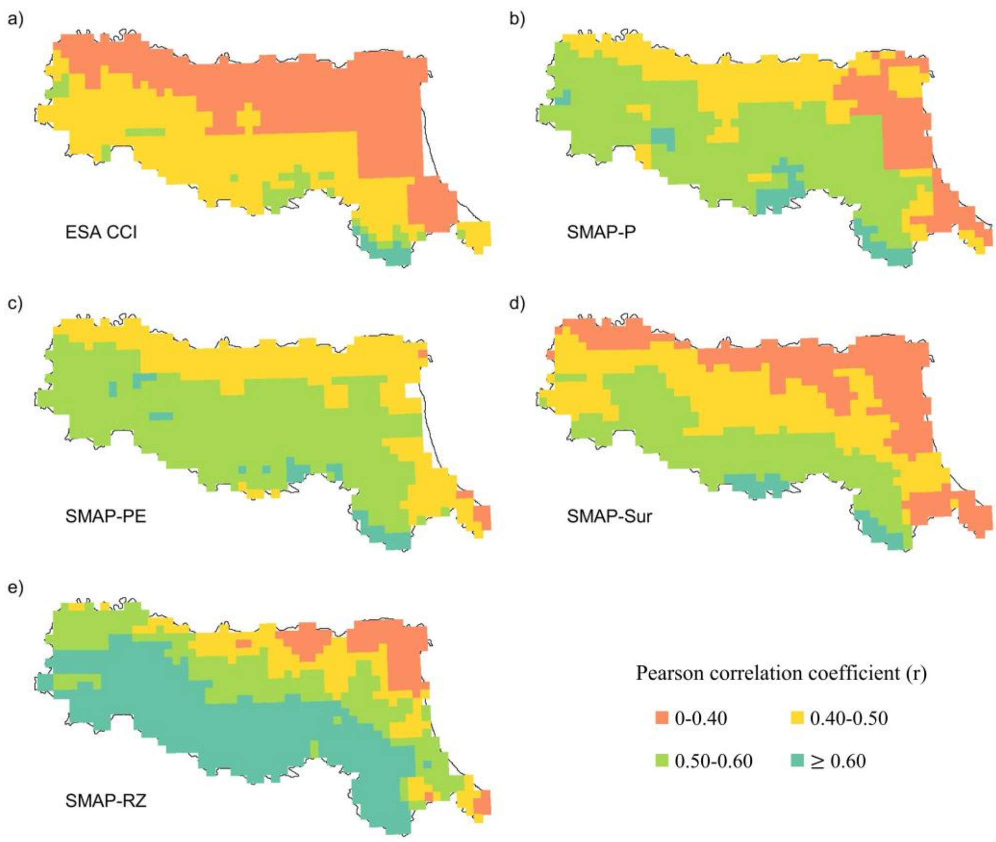

Figure 4. Spatial distribution of the Pearson correlation coefficient (r) between soil moisture and antecedent cumulated rainfall for five satellite soil moisture datasets.

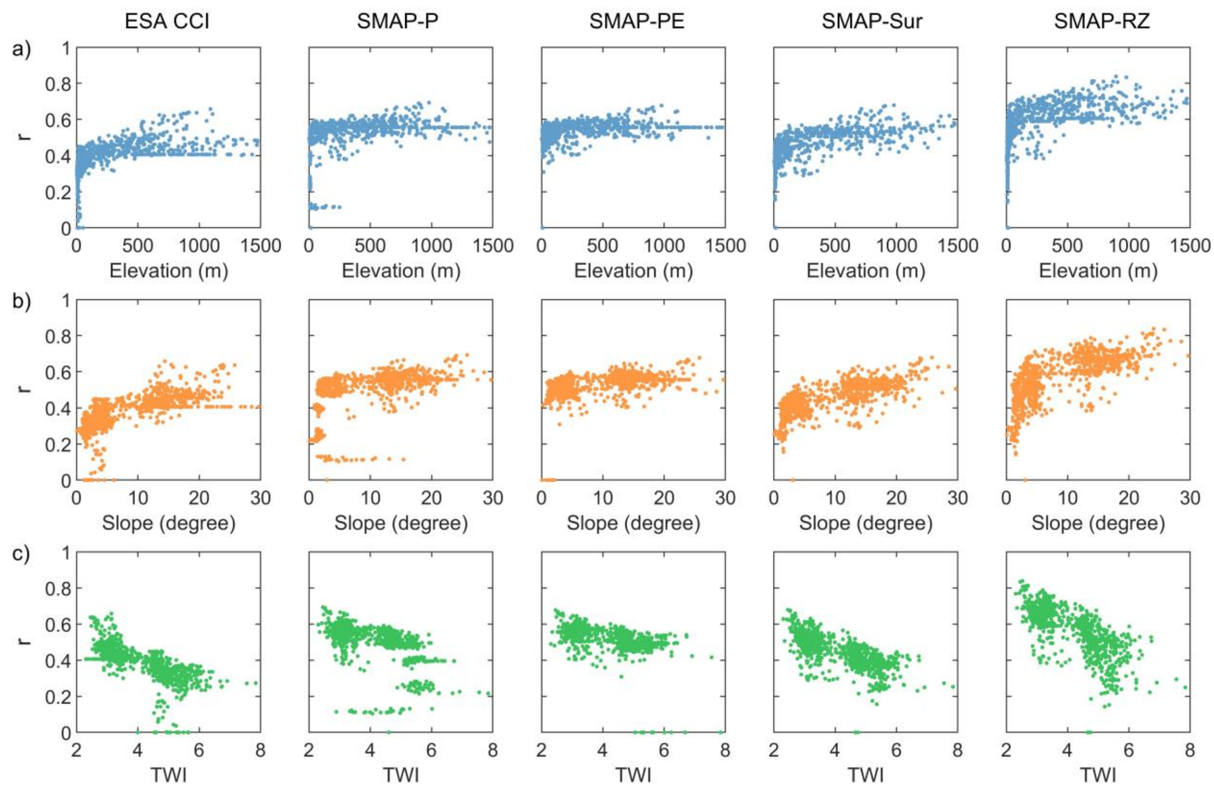

Figure 5. Scatter plots of the Pearson correlation coefficient (r) against topographic indicators (elevation,

slope and TWI) for the five satellite soil moisture datasets.

4.3 The potential in providing valuable information for landslide assessment

To investigate the potential of satellite soil moisture products in providing valuable information for landslide hazard assessments, we first identify infiltration events based on the time series of satellite soil moisture, and explores the significance of event characteristics in landslide occurrence using univariate Bayesian analysis. Only grid cells that have more than 5 landslides within a 5 km radius are selected for analysis in this section. Thus we obtained 21 grid cells and 153 landslides for these grid cells.

The identified infiltration events are visualized in Figure 6 for a sample period (from 1 July 2015 to 30 April 2016) at a sample grid cell (marked with the yellow triangle in Figure 1). During this period, the number of identified infiltration events for ESA CCI, SMAP-Sur and SMAP-RZ are 58, 43 and 32, respectively. The difference in the number of infiltration events is mainly explained by the data characteristics, where SMAP-RZ has a smoother behavior of the soil moisture variation compared with ESA CCI and SMAP-Sur. For the sample grid, there are four infiltration events associated with landslides, with some infiltration events triggering more than one landslide. It is found that these landslides typically occur at a relative wet soil moisture condition or with a sharp increase in soil moisture.

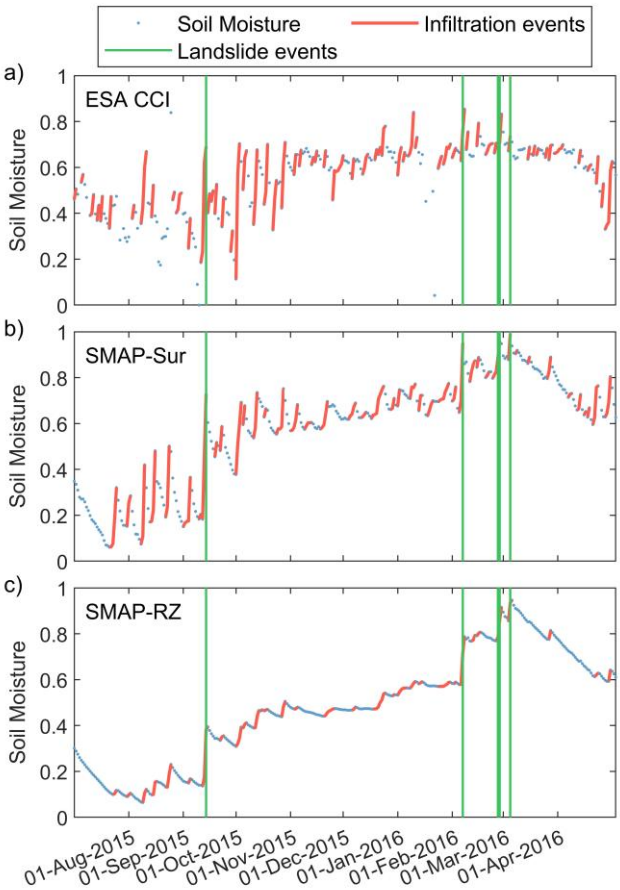

Figure 6. An example of identified infiltration events based on the time series of soil moisture, as well as the corresponding landslides for a) ESA CCI, b) SMAP-Sur and c) SMAP-RZ.

To analyze the characteristics of infiltration events for different satellite soil moisture datasets, the distribution of the infiltration event characteristics is shown in Figure 7. Infiltration events derived from SMAP-RZ have the largest event duration, followed by SMAP-Sur and ESA CCI; while the results for the soil moisture change are opposite: the soil moisture change is smaller for SMAP-RZ than ESA CCI and SMAP-Sur. This is mostly because the effect of rainfall on soil-moisture dynamics is dampened with soil depth. For the start soil moisture, maximum soil moisture and mean soil moisture, there are similar distributions for the satellite soil moisture datasets: ESA CCI has the highest values when the cumulative probability is less than 30%, and SMAP-Sur has the highest values when the cumulative probability is greater than 35%. As for rate of soil moisture change, at the same cumulative probability, ESA CCI has the highest value, followed by SMAP-Sur and then SMAP-RZ. This distribution could be explained by the distribution of the event duration and soil moisture change. These results indicate that there are great differences in infiltration event characteristics between different satellite soil moisture estimates.

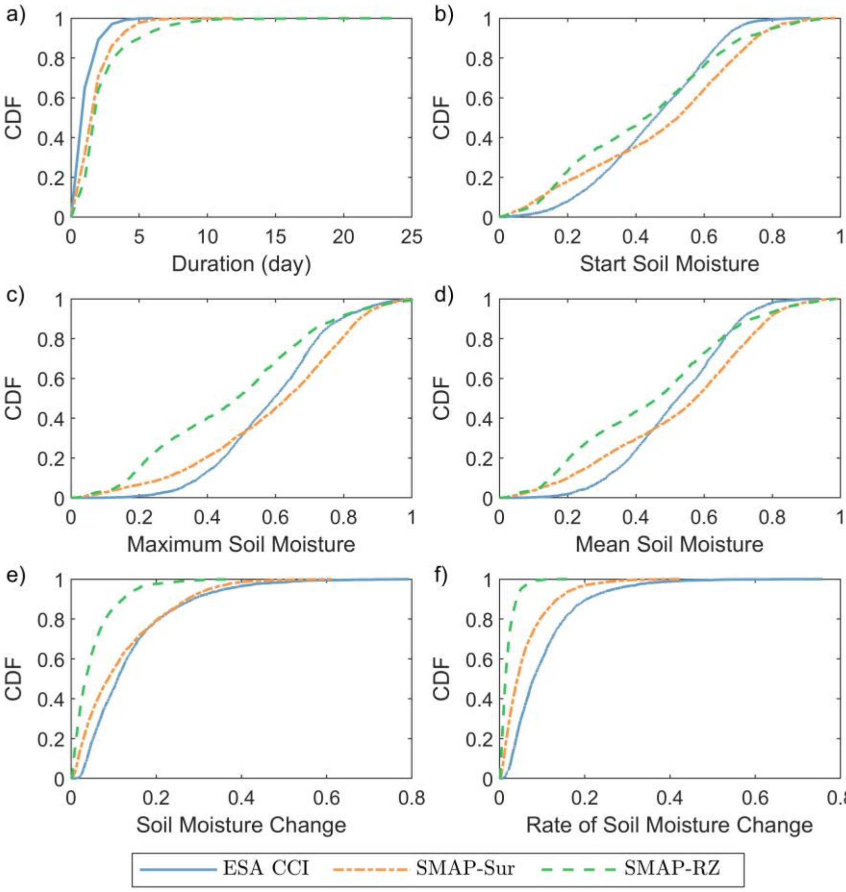

Figure 7. Characteristics of infiltration events derived from different satellite soil moisture datasets.

The significance of the infiltration event characteristics in explaining landslide occurrences is evaluated with univariate Bayesian analysis. Six infiltration event characteristics are tested: infiltration duration, start soil moisture, maximum soil moisture, mean soil moisture, soil moisture change and the rate of soil moisture change. For each event characteristic, its possible values are divided into several intervals according to the variation range. And the conditional probability of landslide occurrence is calculated for every interval. The results of the analysis are shown in Figure 8-10 for ESA CCI, SMAP-Sur and SMAP-RZ respectively. From equation (2), the ratio of $P(I_c|L)$ and $P(I_c)$ (multiplied by $P(L)$) gives the conditional probability of landslide occurrence $P(L|I_c)$. As a result, a large difference between $P(I_c|L)$ and $P(I_c)$ can give high

$P(L|I_c)$ and indicates the high significance of the considered event characteristic.

The results of ESA CCI in Figure 8 clearly show that except for the rate of soil moisture change, there are differences between $P(I_c|L)$ and $P(I_c)$ for other event characteristics. In particular, $P(I_c|L)$ and $P(I_c)$ are markedly different and the corresponding landslide probability $P(L|I_c)$ is well above the prior probability $P(L)$ when the event duration is 5 days, and the start soil moisture, mean soil moisture and soil moisture change are in the interval of 0.6-0.8, and the maximum soil moisture is in the interval of 0.8-1. From the results of SMAP-Sur in Figure 9, for event characteristics other than the rate of soil moisture change, there are differences between $P(I_c|L)$ and $P(I_c)$. And the largest landslide probability $P(L|I_c)$ is obtained when the event duration is between 7-9 days, and other event characteristics are in the highest interval. As for the results of SMAP-RZ in Figure 10, there are differences between $P(I_c|L)$ and $P(I_c)$ for all the event characteristics. When the start soil moisture, maximum soil moisture and mean soil moisture are in the interval of 0.8-1, the corresponding conditional probability of landslide occurrence $P(L|I_c)$ reaches its largest values. When the event duration, soil moisture change and rate of soil moisture change are in the interval of 13-19 days, 0.1-0.3 and 0.03-0.06 respectively, the conditional probability $P(L|I_c)$ is well above the prior probability $P(L)$.

Based on the above results, for the three satellite soil moisture datasets, the conditional probability of landslide occurrence $P(L|I_c)$ is larger than the prior probability $P(L)$, generally when the event characteristics (event duration, start soil moisture, maximum soil moisture, mean soil moisture and soil moisture change) are in their higher intervals, indicating that the five event characteristics of higher values are highly significant in explaining landslide occurrences. This is consistent with the real-life situation, because landslides are more likely to occur when the soil moisture conditions are wetter and the infiltration process lasts longer. In addition, it is interesting to find when the event characteristics are in their higher intervals, the difference between $P(L|I_c)$ and $P(L)$ is more distinct for SMAP-RZ than ESA CCI and SMAP-Sur. This implies that our prior knowledge of the probability of landslide occurrence is better improved by using the 'SMAP-RZ'-derived infiltration events, indicating that SMAP-RZ has greater potential in providing valuable information for landslide hazard assessment compared with the ESA CCI and SMAP-Sur datasets.

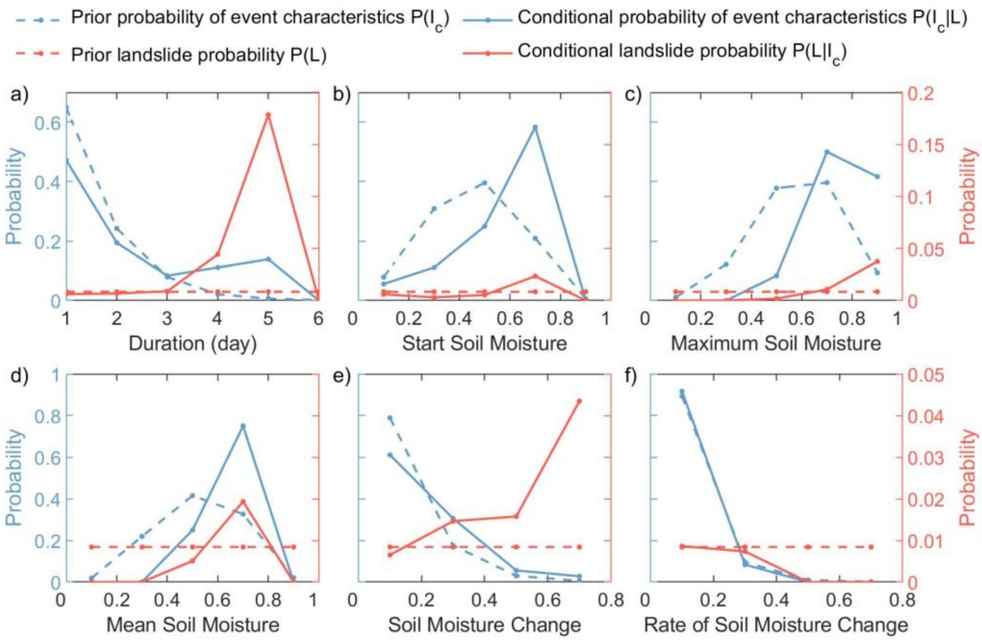

Figure 8. Univariate Bayesian analysis of the infiltration events derived from ESA CCI by considering the event characteristic of a) event duration, b) start soil moisture, c) maximum soil moisture, d) mean soil moisture, e) soil moisture change and f) rate of soil moisture change.

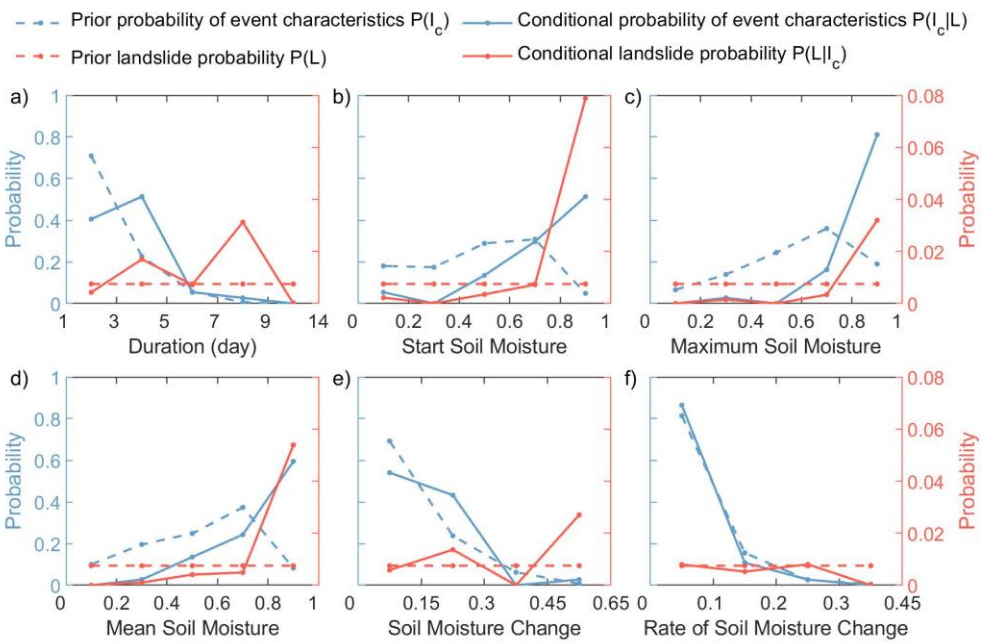

Figure 9. Univariate Bayesian analysis of the infiltration events derived from SMAP-Sur by considering the event characteristic of a) event duration, b) start soil moisture, c) maximum soil moisture, d) mean soil moisture, e) soil moisture change and f) rate of soil moisture change.

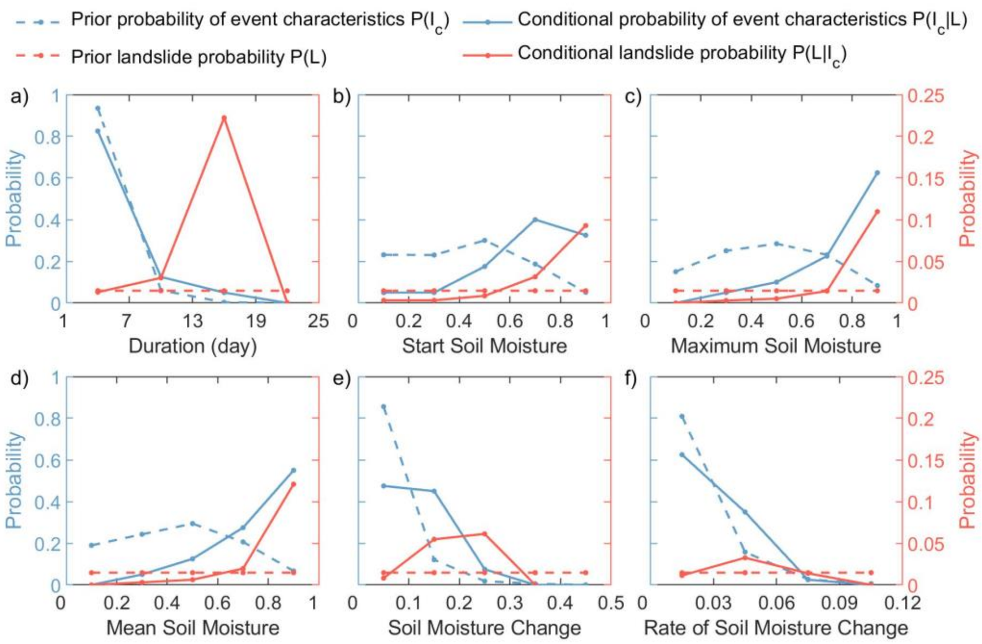

Figure 10. Univariate Bayesian analysis of the infiltration events derived from SMAP-RZ by considering the event characteristic of a) event duration, b) start soil moisture, c) maximum soil moisture, d) mean soil moisture, e) soil moisture change and f) rate of soil moisture change.

5. Discussion

5.1 Identification of infiltration events

Based on the time series of satellite soil moisture, the infiltration events are identified using an automatic algorithm, which requires the determination of two thresholds T_1 and T_2. In this study, T_1 and T_2 are determined as their 10th percentiles. One question that arises is whether the value of thresholds has effect on the identified infiltration events and the results of Bayesian analysis. Taking the SMAP-RZ dataset as an example, we identify infiltration events by determining thresholds as the 5th, 15th and 20th percentiles, respectively, and carried out the corresponding Bayesian analysis. The results of Bayesian analysis are very similar for all the six event characteristics, and we chose the results of the event duration and mean soil moisture to show in Figure 11 and Table 2. As is seen, for the two event characteristics, the pattern of the probability distribution is very similar for all test thresholds. The only difference exhibits in the magnitude of the probability, and the difference is very small (Table 2). By comparing the results of different satellite soil moisture datasets, it is found that the limited difference caused by the threshold values has little effect on the comparison results, where the characteristics of 'SMAP-RZ'-derived infiltration events could greatly improve our prior knowledge of the probability of landslide occurrence. It should be noted that this conclusion is limited to the case where the thresholds vary from 0 to their 20th percentiles. In addition, although the threshold values have little effect on the results of Bayesian analysis, they do influence the total number of infiltration events: the total number of infiltration events decreases as the threshold values become larger. Therefore, for other applications of the infiltration events, for example, the prediction of landslides, the threshold values may affect the results, and more attention should be paid to the selection of the thresholds. Clearly more studies are needed to verify this assumption.

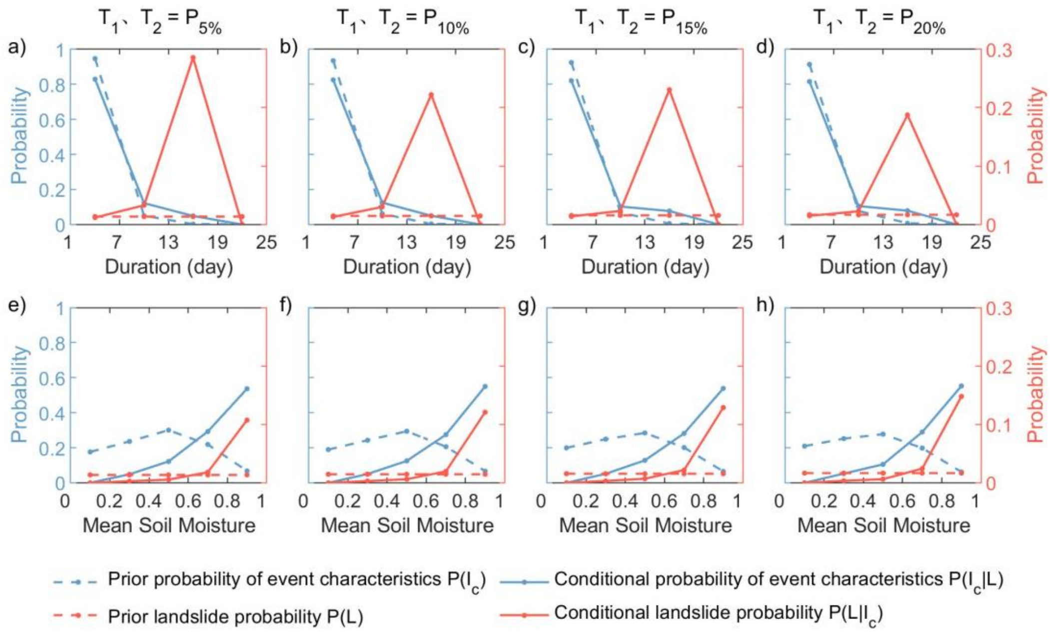

Figure 11. Univariate Bayesian analysis of the infiltration events identified based on different threshold values.

Table 2a. Results of Bayesian analysis for the event characteristic of the duration by considering different thresholds.

Threshold 1	Threshold 2	P(L)	$P(L|I_c)$, I_c:Duration			
			[1,7)	[7,13)	[13,19)	[19,25]
$P_{5\%}$	$P_{5\%}$	0.014	0.012	0.033	0.286	0
$P_{10\%}$	$P_{10\%}$	0.015	0.013	0.030	0.222	0
$P_{15\%}$	$P_{15\%}$	0.016	0.014	0.023	0.231	0
$P_{20\%}$	$P_{20\%}$	0.017	0.015	0.023	0.188	0

Table 2b. Results of Bayesian analysis for the event characteristic of mean soil moisture by considering different thresholds.

Threshold 1	Threshold 2	P(L)	$P(L|I_c)$, I_c: Mean Soil Moisture				
			[0,0.2)	[0.2,0.4)	[0.4,0.6)	[0.6,0.8)	[0.8,1]
$P_{5\%}$	$P_{5\%}$	0.014	0	0.003	0.006	0.018	0.107
$P_{10\%}$	$P_{10\%}$	0.015	0	0.003	0.006	0.020	0.121
$P_{15\%}$	$P_{15\%}$	0.016	0	0.003	0.007	0.022	0.129
$P_{20\%}$	$P_{20\%}$	0.017	0	0.003	0.006	0.024	0.148

5.2 Advantages of the SMAP L4 product

To gain a better understanding of the difference between different satellite soil moisture datasets in landslide assessment potential, we evaluate the satellite soil moisture products based on three aspects: (1) the applicability in practical applications in terms of data completeness; (2) the relationship with the commonly used rainfall information in landslide predictions; (3) the potential to provide valuable information for landslide hazard assessment.

For the completeness evaluation, SMAP L4 product (including the SMAP-Sur and SMAP-RZ datasets) do not have any missing values, hence are beneficial to analyzing the temporal variations of soil moisture and monitoring the landslide occurrence. The correlation between soil moisture and antecedent cumulated rainfall shows that SMAP-Sur and SMAP-RZ have more rational spatial distribution of the Pearson correlation coefficients compared with other datasets, which can be better explained by the distribution of slope and TWI. As for the performance in providing valuable information for landslide hazard assessment, the results of Bayesian analysis indicate that our prior knowledge of the probability of landslide occurrence is better improved by using the 'SMAP-RZ'-derived infiltration events, compared with the ESA CCI and SMAP-Sur dataset.

In summary, the SMAP L4 product, especially the SMAP-RZ dataset, performs better in our evaluation studies, indicating greater potential to be used in landslide assessment in the study region. There are several potential reasons for such an outcome. First, SMAP L4 is a modeled product, it is not expected to have any gaps in the time series. Second, from the published studies on the evaluation of satellite soil moisture products, the SMAP L4 product shows higher accuracy with in-situ measurements (Al-Yaari et al. 2019; Reichle et al. 2017). And it is inferred that the better performance of the SMAP L4 product benefits from its processing algorithm, which assimilates SMAP L-band brightness temperature measurements and precipitation observations into the NASA Catchment land surface model. The higher accuracy of the SAMP L4 product may explain the better correlation relationship of SMAP-RZ and SMAP-Sur with the antecedent cumulated rainfall, in terms of the more rational spatial distribution. Third, considering that shallow landslides typically occur at depth deeper than the uppermost 5 cm, the greater the depth of soil moisture measurement, the better it can represent the actual hydrologic response that triggers landslides(Marino et al. 2020). Therefore, it is not surprising that SMAP-RZ performs better in providing valuable information for landslide occurrence. Besides, as the landslide assessment potential of satellite soil moisture is evaluated by taking advantage of infiltration events, a smoother signal of SMAP-RZ time series allows easier identification of the significant infiltration events.

In addition to the above superior performance of SMAP-RZ to other datasets, SMAP-RZ also shows advantages in landslide predictions compared with the commonly used rainfall information. As landslide occurrence is related to the increase of pore water pressure and the decrease of matric suction that are caused by the infiltration process, characterizing infiltration events based on soil moisture estimates provides a more direct way of landslide occurrence identification than using rainfall information. Besides, the high-frequency rainfall data is too "noisy" relative to the dampened signal of root zone soil moisture that is provided by SMAP-RZ. Therefore, SMAP-RZ can better capture the timescale of infiltration events related to landslides.

5.3 Methodological limitations

Specific limitations arise from the use of normalized soil moisture data. Although the normalized data facilitates the analysis, it has no physical meaning other than the relative wet condition, which makes it difficult to see the difference in data for different locations. An improvement in this respect could be the derivation of the soil saturation, which needs measurements of the porosity and the saturated and residual water content at each location; however, such information is usually unavailable.

When carrying out the correlation study between the satellite soil moisture and the antecedent cumulated rainfall, we only use three topographic indicators (elevation, slope and TWI) to explain the spatial distribution of the correlation coefficients. However, there are other factors that can affect the spatial distribution of soil moisture, such as soil texture and vegetation (Gómez-Plaza et al. 2001), which may also have influence on the spatial distribution of the correlation coefficients. Therefore, a detailed analysis will be carried out in our future studies.

Furthermore, Bayesian analysis is limited by the completeness of landslide data. The landslide records used in this study are based on human experiences (e.g. reports, national and local press, technical documents, etc.), thus small events with less damage to humans or infrastructure are likely to be unreported. Besides, as the infiltration events with landslides are truncated on the day the landslide occurs, the date-based landslide timing may introduce uncertainties to the event characteristics. Consequently, the results of Bayesian analysis could be biased.

Finally, through the identification of the infiltration events based on satellite soil moisture and the analysis of the significance of event characteristics in landslide occurrence, we can quantitatively evaluate the landslide assessment potential of different satellite soil moisture products. In addition to the evaluation application as shown in this study, the derived infiltration events have the potential to be used in landslide hazard assessment such as for landslide predictions, and therefore further explorations in this are encouraged.

6. Conclusions

In this study, we assess the potential of different satellite soil moisture products in landslide hazard assessment in the Emilia-Romagna region, using the ESA CCI soil moisture dataset, the SMAP Level-3 (L3), enhanced Level-3 (L3), Level-4 (L4) surface, and Level-4 (L4) root zone soil moisture datasets. It is found that the SMAP L4 product, especially the SMAP-RZ dataset, performs better in this comparative study. Specifically, the SMAP L4 product has no missing values, while SMAP L3 product has intermittent missing values, unfeasible for analyzing the temporal variations of soil moisture. The correlation between the soil moisture and the antecedent cumulated rainfall shows that for the SMAP L4 product, the spatial distribution of the correlation coefficients can be better explained by the distribution of slope and TWI. As for the performance in providing valuable information for landslide hazard assessment, Bayesian analysis on the infiltration events indicates that our prior knowledge of the probability of landslide occurrence is better improved by using the 'SMAP-RZ'-derived infiltration events, compared with the ESA CCI and SMAP-Sur dataset.

In summary, it can be concluded that the SMAP L4 root zone soil moisture has a greater potential to be used for landslide hazard assessment in the study area. In order to make the conclusion more general, more researches are needed using other soil moisture datasets and evaluation methods. For instance, the collection of in-situ soil moisture measurements will be critical to carry out further evaluations by comparing the satellite soil moisture products with the ground-based measurements.

Acknowledgements

The authors acknowledge Dr. Matteo Berti for providing landslides data and Arpae Emilia-Romagna organization for providing the rain gauge measurements. This study is supported by Project funded by China Postdoctoral Science Foundation (Nos. 2020M681660) and National Natural Science Foundation of China (Nos. 41871299).

References

Al-Yaari, A., Wigneron, J.P., Dorigo, W., Colliander, A., Pellarin, T., Hahn, S., Mialon, A., Richaume, P., Fernandez-Moran, R., Fan, L., Kerr, Y.H., & De Lannoy, G., 2019. Assessment and inter-comparison of recently developed/reprocessed microwave satellite soil moisture products using ISMN ground-based measurements. *Remote Sensing of Environment, 224*, 289-303

Beven, K.J., & Kirkby, M.J., 1979. A physically based, variable contributing area model of basin hydrology/Un modèle à base physique de zone d'appel variable de l'hydrologie du bassin versant.

Hydrological Sciences Journal, 24, 43-69

Brocca, L., Ciabatta, L., Moramarco, T., Ponziani, F., Berni, N., & Wagner, W., 2016. Use of satellite soil moisture products for the operational mitigation of landslides risk in central Italy. *Satellite Soil Moisture Retrieval* (pp. 231-247): Elsevier

Cui, C., Xu, J., Zeng, J., Chen, K.-S., Bai, X., Lu, H., Chen, Q., & Zhao, T., 2017. Soil Moisture Mapping from Satellites: An Intercomparison of SMAP, SMOS, FY3B, AMSR2, and ESA CCI over Two Dense Network Regions at Different Spatial Scales. *Remote Sensing, 10*

Dorigo, W., Wagner, W., Albergel, C., Albrecht, F., Balsamo, G., Brocca, L., Chung, D., Ertl, M., Forkel, M., & Gruber, A., 2017. ESA CCI Soil Moisture for improved Earth system understanding: State-of-the art and future directions. *Remote Sensing of Environment, 203*, 185-215

Felsberg, A., De Lannoy, G.J.M., Girotto, M., Poesen, J., Reichle, R.H., & Stanley, T., 2021. Global Soil Water Estimates as Landslide Predictor: The Effectiveness of SMOS, SMAP, and GRACE Observations, Land Surface Simulations, and Data Assimilation. *Journal of Hydrometeorology, 22*, 1065-1084

Gariano, S.L., Melillo, M., Peruccacci, S., & Brunetti, M.T., 2019. How much does the rainfall temporal resolution affect rainfall thresholds for landslide triggering? *Natural Hazards, 100*, 655-670

Glade, T., Crozier, M., & Smith, P., 2000. Applying probability determination to refine landslide-triggering rainfall thresholds using an empirical "Antecedent Daily Rainfall Model". *Pure and Applied Geophysics, 157*, 1059-1079

Godt, J.W., Baum, R.L., & Chleborad, A.F., 2006. Rainfall characteristics for shallow landsliding in Seattle, Washington, USA. *Earth surface processes and landforms, 31*, 97-110

Gómez-Plaza, A., Martınez-Mena, M., Albaladejo, J., & Castillo, V., 2001. Factors regulating spatial distribution of soil water content in small semiarid catchments. *Journal of Hydrology, 253*, 211-226

Lagomarsino, D., Segoni, S., Fanti, R., & Catani, F., 2012. Updating and tuning a regional-scale landslide early warning system. *Landslides, 10*, 91-97

Ma, H., Zeng, J., Chen, N., Zhang, X., Cosh, M.H., & Wang, W., 2019. Satellite surface soil moisture from SMAP, SMOS, AMSR2 and ESA CCI: A comprehensive assessment using global ground-based observations. *Remote Sensing of Environment, 231*

Marino, P., Peres, D.J., Cancelliere, A., Greco, R., & Bogaard, T.A., 2020. Soil moisture information can improve shallow landslide forecasting using the hydrometeorological threshold approach. *Landslides, 17*, 2041-2054

Mirus, B., Morphew, M., & Smith, J., 2018a. Developing Hydro-Meteorological Thresholds for Shallow Landslide Initiation and Early Warning. *Water, 10*

Mirus, B.B., Becker, R.E., Baum, R.L., & Smith, J.B., 2018b. Integrating real-time subsurface hydrologic monitoring with empirical rainfall thresholds to improve landslide early warning. *Landslides, 15*, 1909-1919

Monerris, A., Schmugge, T., & Jedlovec, G., 2009. Soil moisture estimation using L-band radiometry. *Advances in Geoscience and Remote Sensing*

Naidu, S., Sajinkumar, K.S., Oommen, T., Anuja, V.J., Samuel, R.A., & Muraleedharan, C., 2018. Early warning system for shallow landslides using rainfall threshold and slope stability analysis. *Geoscience Frontiers, 9*, 1871-1882

Piciullo, L., Calvello, M., & Cepeda, José M., 2018. Territorial early warning systems for rainfall-induced landslides. *Earth-Science Reviews, 179*, 228-247

Piepmeier, J.R., Focardi, P., Horgan, K.A., Knuble, J., Ehsan, N., Lucey, J., Brambora, C., Brown, P.R., Hoffman, P.J., French, R.T., Mikhaylov, R.L., Kwack, E.Y., Slimko, E.M., Dawson, D.E., Hudson, D., Peng, J., Mohammed, P.N., De Amici, G., Freedman, A.P., Medeiros, J., Sacks, F., Estep, R., Spencer, M.W., Chen, C.W., Wheeler, K.B., Edelstein, W.N., O'Neill, P.E., & Njoku, E.G., 2017. SMAP L-Band Microwave Radiometer: Instrument Design and First Year on Orbit. *IEEE Trans Geosci Remote Sens, 55*, 1954-1966

Reichle, R.H., De Lannoy, G.J., Liu, Q., Ardizzone, J.V., Colliander, A., Conaty, A., Crow, W., Jackson, T.J., Jones, L.A., & Kimball, J.S., 2017. Assessment of the SMAP level-4 surface and root-zone soil moisture product using in situ measurements. *Journal of Hydrometeorology, 18*, 2621-2645

Rosi, A., Peternel, T., Jemec-Auflič, M., Komac, M., Segoni, S., & Casagli, N., 2016. Rainfall thresholds for rainfall-induced landslides in Slovenia. *Landslides, 13*, 1571-1577

Segoni, S., Rosi, A., Fanti, R., Gallucci, A., Monni, A., & Casagli, N., 2018. A Regional-Scale Landslide Warning System Based on 20 Years of Operational Experience. *Water, 10*

Thomas, M.A., Collins, B.D., & Mirus, B.B., 2019. Assessing the Feasibility of Satellite-Based Thresholds for Hydrologically Driven Landsliding. *Water Resources Research, 55*, 9006-9023

Thomas, M.A., Mirus, B.B., & Smith, J.B., 2020. Hillslopes in humid-tropical climates aren't always wet: Implications for hydrologic response and landslide initiation in Puerto Rico. *Hydrological Processes, 34*, 4307-4318

Wicki, A., Lehmann, P., Hauck, C., Seneviratne, S.I., Waldner, P., & Stähli, M., 2020. Assessing the potential of soil moisture measurements for regional landslide early warning. *Landslides, 17*, 1881-1896

Zhao, B., Dai, Q., Han, D., Dai, H., Mao, J., & Zhuo, L., 2019. Probabilistic Thresholds for Landslides Warning by Integrating Soil Moisture Conditions with Rainfall Thresholds. *Journal of Hydrology*

Zhao, B., Dai, Q., Han, D., Zhang, J., Zhuo, L., & Berti, M., 2020. Application of hydrological model simulations in landslide predictions. *Landslides, 17*, 877-891

Zhuo, L., Dai, Q., Han, D., Chen, N., & Zhao, B., 2019a. Assessment of Simulated Soil Moisture from WRF Noah, Noah-MP, and CLM Land Surface Schemes for Landslide Hazard Application. *Hydrology and Earth System Sciences Discussions*, 1-48

Zhuo, L., Dai, Q., Han, D., Chen, N., Zhao, B., & Berti, M., 2019b. Evaluation of Remotely Sensed Soil Moisture for Landslide Hazard Assessment. *IEEE Journal of Selected Topics in Applied Earth Observations and Remote Sensing, 12*, 162-173

List of Figure Captions

Figure 1. Map of the Emilia-Romagna region and the location of reference grid centers, landslides, and the grid center for infiltration event analysis.

Figure 2. Boxplot representations of the median (red line), upper and lower quartiles (box), 1.5Â interquartile range (whiskers) and outliers (black dots) for missing values at all the reference grid cells for the period from 1 April 2015 to 31 December 2019.

Figure 3. Boxplot representations of the median (red line), upper and lower quartiles (box), 1.5Â interquartile range (whiskers) and outliers (black dots) for the Pearson correlation coefficient (r) between soil moisture and antecedent cumulated rainfall at all the reference grid cells.

Figure 4. Spatial distribution of the Pearson correlation coefficient (r) between soil moisture and antecedent cumulated rainfall for five satellite soil moisture datasets.

Figure 5. Scatter plots of the Pearson correlation coefficient (r) against topographic indicators (elevation, slope and TWI) for the five satellite soil moisture datasets.

Figure 6. An example of identified infiltration events based on the time series of soil moisture, as well as the corresponding landslides for a) ESA CCI, b) SMAP-Sur and c) SMAP-RZ.

Figure 7. Characteristics of infiltration events derived from different satellite soil moisture datasets.

Figure 8. Univariate Bayesian analysis of the infiltration events derived from ESA CCI by considering the event characteristic of a) event duration, b) start soil moisture, c) maximum soil moisture, d) mean soil

moisture, e) soil moisture change and f) rate of soil moisture change.

Figure 9. Univariate Bayesian analysis of the infiltration events derived from SMAP-Sur by considering the event characteristic of a) event duration, b) start soil moisture, c) maximum soil moisture, d) mean soil moisture, e) soil moisture change and f) rate of soil moisture change.

Figure 10. Univariate Bayesian analysis of the infiltration events derived from SMAP-RZ by considering the event characteristic of a) event duration, b) start soil moisture, c) maximum soil moisture, d) mean soil moisture, e) soil moisture change and f) rate of soil moisture change.

Figure 11. Univariate Bayesian analysis of the infiltration events identified based on different threshold values.